# Supporting Information

## Mid- and far-infrared localized surface plasmon resonances in chalcogen-hyperdoped Si

Mao Wang[1,*], Ye Yu[2,‡], Slawomir Prucnal[1], Yonder Berencén[1], Mohd Saif Shaikh[1], Lars Rebohle[1], Muhammad Bilal Khan[1], Vitaly Zviagin[3], René Hübner[1], Alexej Pashkin[1], Artur Erbe[1], Yordan Georgiev[1], Marius Grundmann[3], Manfred Helm[1,4], Robert Kirchner[2,5] and Shengqiang Zhou[1]

[1]Helmholtz-Zentrum Dresden-Rossendorf, Institute of Ion Beam Physics and Materials Research, Bautzner Landstraße 400, 01328 Dresden, Germany

[2]Institute of Semiconductors and Microsystems, Technische Universität Dresden, 01062 Dresden, Germany

[3]Felix-Bloch-Institut für Festkörperphysik, Universität Leipzig, Linnéstraße 5, 04103 Leipzig, Germany

[4]Institut für Angewandte Physik (IAP), Technische Universität Dresden, 01062 Dresden, Germany

[5]Cluster of Excellence Centre for Advancing Electronics Dresden (CfAED), Technische Universität Dresden, 01062 Dresden, Germany

Corresponding authors, email: *m.wang@hzdr.de; ‡ye.yu@tu-dresden.de.

## A. Sample preparation methods

After ion implantation, the as-implanted Si wafers were annealed by millisecond flash-lamp annealing (FLA). A homogeneous flash-light pulse was provided by the installed array of Xe-lamps connected in parallel with a reflector behind and a pre-heating module. Prior to the flash, the as-implanted samples were firstly preheated to a temperature of 400 $^{o}$C for 30 s in nitrogen atmosphere. Subsequently, the samples were annealed by FLA with a fixed pulse duration of 3 ms and an energy density of 58 J/cm$^2$. This corresponds to a temperature between 1100 and 1300 °C at the sample surface. Further details of the FLA system employed in our experiments can be found elsewhere [1-3].

The antenna patterning was achieved by electron-beam lithography and reactive ion etching. Electron beam lithography (Raith e_LiNE plus, Raith GmbH) was performed using an Extra High-voltage Transformer (EHT) at 30 kV. Hydrogen silsesquioxane (HSQ) resist was spun onto the samples with a thickness of 200 nm. After patterning, the HSQ resist was developed using a diluted tetramethyl ammonium hydroxide (TMAH)-based solution at 23 ˚C for 15 s. The samples were then etched in an inductively coupled plasma (ICP) reactive-ion-etch system (Facility SI 591, SENTECH Instruments GmbH) using $SF_6$ and $CF_4$ gases in a mixed process. A laser end-point detection system was used to stop the process once the etched depth exceeded the thickness of the entire doped layer (etched thickness is around 300 nm). Finally, the resist was stripped using hydrogen fluoride (HF) aqueous solution.

## B. Electromagnetic simulations

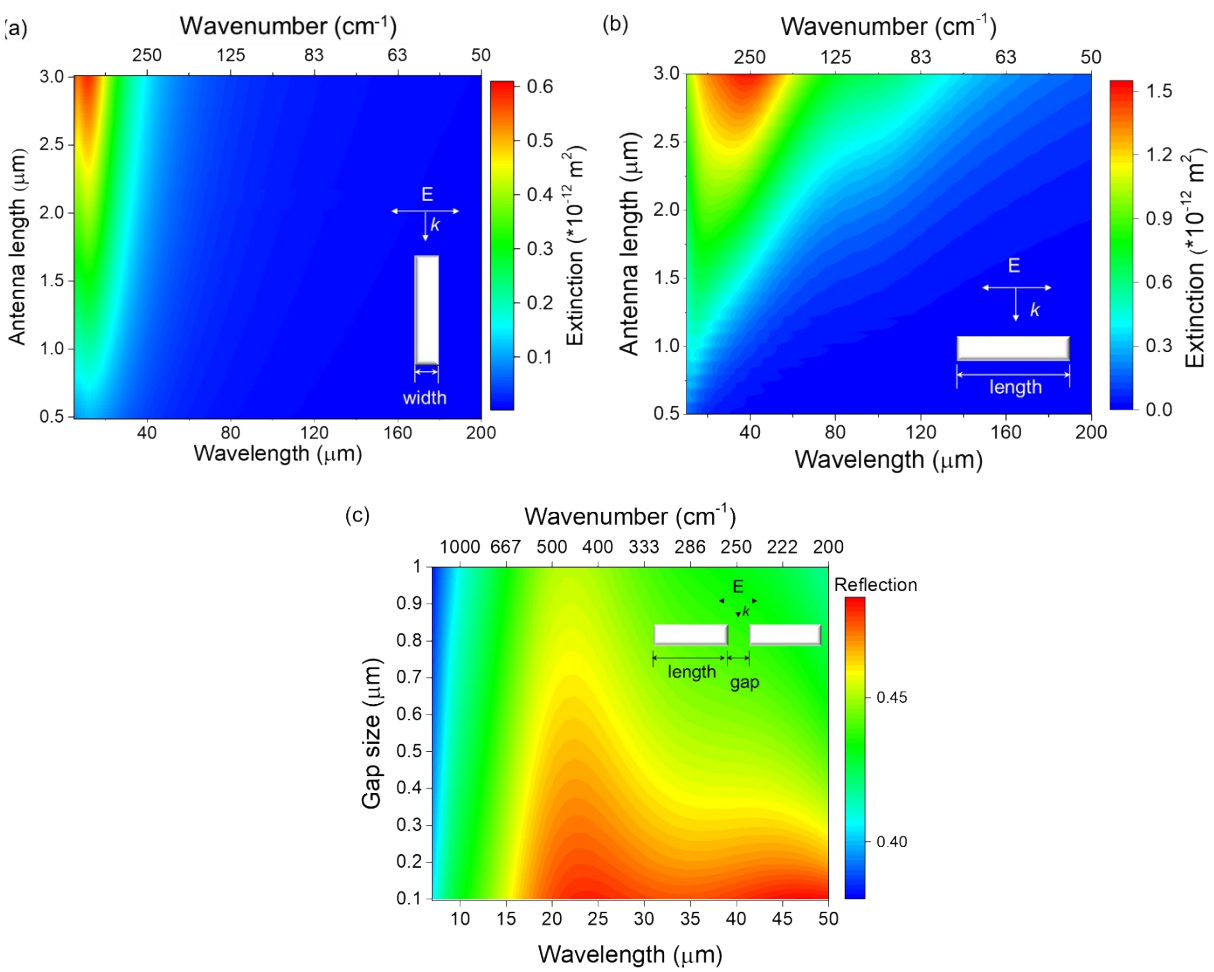


FIG. S1. Simulated extinction plotted as a function of wavelength as a function of the antenna length of a single-arm antenna with the electric field polarization perpendicular to the long antenna axis (a) and parallel to the long antenna axis (b). (c) Simulated reflection spectra as a function of the arm gap size in an array of paired-arm antennas (antenna arm length of 2 μm) with the electric field polarization parallel to the long antenna axis.

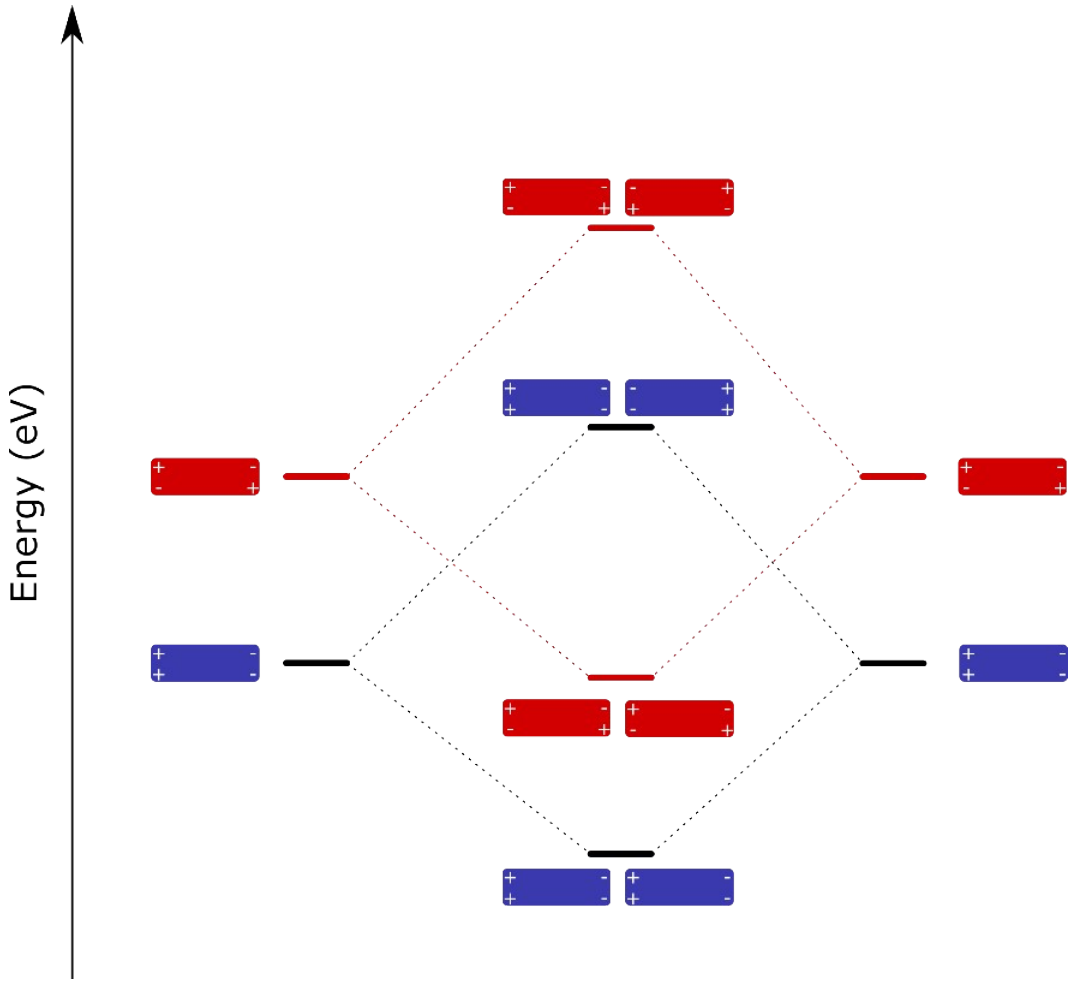


FIG. S2. Illustration of the plasmonic hybridization of the dipolar and quadrupolar resonances. The blue set of nanostructures represent the hybridization in between dipolar resonances; whereas the red set the quadrupolar resonances.

## C. Infrared spectra of the antenna arrays

Figures S3 and S4 show representative reflection spectra for antenna arrays with an antenna length of $l$ = 2.0 μm, a width of $w$ = 0.8 μm, and a gap size $g$ varying from 0.2 μm to 1 μm.

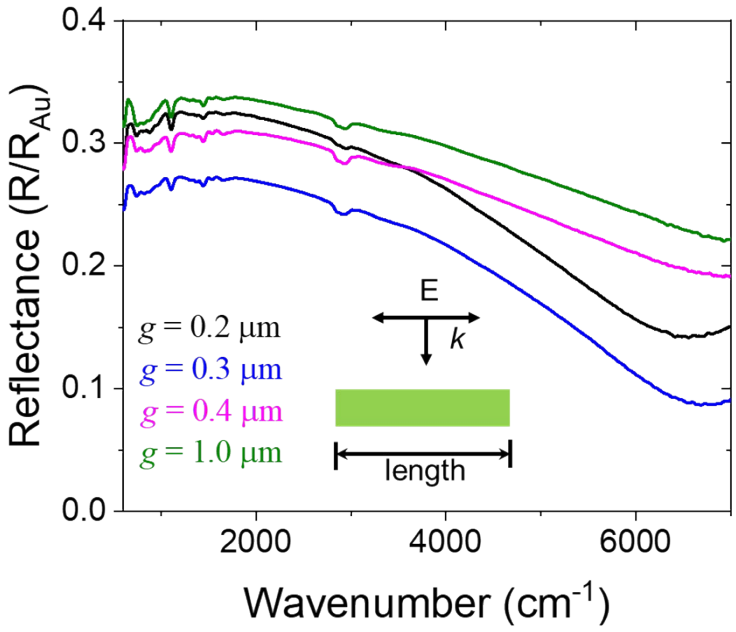


FIG. S3. Representative reflection spectra for antenna arrays with an antenna length of $l$ = 2.0 μm, a width of $w$ = 0.8 μm, and a gap size g varying from 0.2 μm to 1 μm. The spectra are recorded by FTIR spectroscopy in the mid-infrared range at normal incidence with the electric field polarization direction parallel to the long antenna axis.

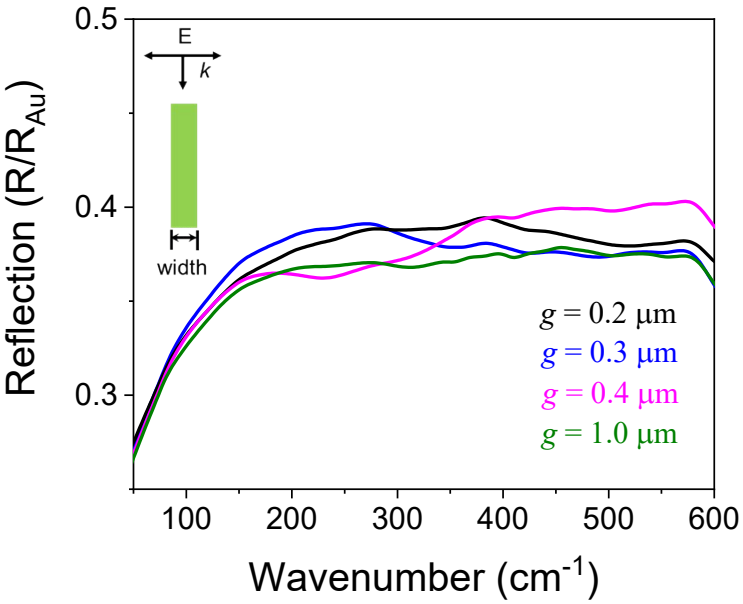


FIG. S4. Representative reflection spectra for antenna arrays with an antenna length of $l$ = 2.0 μm, a width of $w$ = 0.8 μm, and a gap size g varying from 0.2 μm to 1 μm. The spectra are recorded by FTIR spectroscopy at normal incidence with the electric field polarization direction perpendicular to the long antenna axis.

## D. Material properties

Table I. The electrical properties of FLA-treated Te-hyperdoped Si layers with a peak doping concentration of 1.5%. The effective carrier concentration and the Hall mobility are measured at room temperature.

| Sample ID | Tellurium peak Concentration ($cm^{-3}$) | Sheet carrier density ($10^{15}/cm^3$) | Electron mobility ($cm^2/V{\cdot}s$) |
|---|---|---|---|
| Te-1.5%_A (in the main text) | 1.5 (%); $7.5 \times 10^{20}$ $cm^{-3}$ | 1.50 | 31.73 |
| Te-1.5%_B | 1.5 (%); $7.5 \times 10^{20}$ $cm^{-}$ | 1.47 | 34.62 |
| Te-1.5%_C | 1.5 (%); $7.5 \times 10^{20}$ $cm^{-}$ | 1.61 | 30.55 |
| Te-1.5%_D | 1.5 (%); $7.5 \times 10^{20}$ $cm^{-}$ | 1.44 | 35.57 |


[1] W. Skorupa, T. Gebel, R. A. Yankov, S. Paul, W. Lerch, D. F. Downey, and E. A. Arevalo, Advanced thermal processing of ultrashallow implanted junctions using flash lamp annealing, J. Electrochem. Soc. **152**, G436 (2005).

[2] R. McMahon, M. Smith, K. Seffen, M. Voelskow, W. Anwand, and W. Skorupa, Flash-lamp annealing of semiconductor materials—Applications and process models, Vacuum **81**, 1301 (2007).

[3] S. Zhou, F. Liu, S. Prucnal, K. Gao, M. Khalid, C. Baehtz, M. Posselt, W. Skorupa, and M. Helm, Hyperdoping silicon with selenium: solid vs. liquid phase epitaxy, Sci. Rep. **5**, 8329 (2015).